Nigerian Journal of Physics (NJP)
ISSN: 1595-0611
Volume 32(2), June 2023

Low Latitude Ionospheric *foF2* Variability and F2-Region Virtual Height Response During Low Solar Activity

***[1]Ehinlafa, O. E, [2]Àlàgbé, G. A, [3]Onanuga, O. K. and [4]Adeniyi, J. O.**

[1]Department of Physics, University of Ilorin, Ilorin, Nigeria
[2]Department of Pure & Applied Physics, Ladoke Akintola University of Technology, Ogbomoso, Nigeria
[3]Department of Physical Sciences, Lagos State University of Science and Technology, Ikorodu, Nigeria
[4]Private Individual, Pipeline Road, Ilorin, Nigeria

[*]Corresponding author's email: segunolu74@gmail.com Phone: +2348034343563
ORC-ID: 0009-0008-3982-8274

ABSTRACT
Diurnal, seasonal and annual critical frequency relative deviation index and virtual height (*h'F2)* response of F2-region ionosphere was studied during a low solar activity over Ilorin (latitude 8.31°N, longitude 4.34°E, dip latitude 2.95°), a low latitude station along the equatorial anomaly trough. The relative deviation index and mean were used for the analysis of critical frequency ***(****f_oF2****)*** and virtual height (*h'F2*) respectively. The least relative deviation index (2-17%) was obtained during the day; it increased at night (8-55%); the highest value obtained during pre-sunrise (17-68%), for the period of low solar activity. Two main peaks were noticed in relative deviation index and virtual height: the pre-sunrise peak, which is higher, and the post-sunset peak. Annually, relative deviation index and virtual height peak at 44% and 275 km respectively, for the pre-sunrise period; and at 37% and 295 km respectively, for the post-sunset period, during the low solar activity. In general, the value of the pre-sunrise peak is higher than that of the post-sunset peak for both relative deviation index and virtual height during the entire season.

Keywords:
Critical frequency (f_oF2),
Relative Deviation Index (V_R),
Virtual Height (h'F2),
Low Solar Activity (LSA).

INTRODUCTION

Ionospheric F2-region has been shown to be the most expeditious region for long-distance high frequency (HF) radio propagation. It is characterised by the critical frequency (f_oF2) and the peak height of the electron density (h_mF2). This region is better understood and interpreted by radio propagation experts. A keen prediction of the f_oF2 relative deviation index in relation with the peak height of the electron density (h_mF2) and virtual height (*h'F2*) occurrence is thus of great advantage in this respect as it constitutes a remarkable property of the complex theme of space weather, for both its practical utilization and scientific value. Various researchers, such as, Akala *et al.* (2011), Bilitza *et al.* (2004), Olawepo and Adeniyi (2012) and Jayachandran *et al.* (1995), have studied, at different latitudes and solar cycles, the f_oF2 spread. The electron density statistical distribution at fixed heights was studied by Oladipo *et al*. (2009) using the Gaussian distribution test. Also, f_oF2 variability pattern at different latitudes using GPS observations was carried out by Jin *et al*. (2008) and Lilensten and Blelly (2002). At mid-latitudes, Zhang and Holt (2008) investigated electron density variability and plasma temperatures.

This work considered the diurnal, seasonal, and annual *foF2* variability for a single low latitude station of Ilorin in West Africa region (latitude 8.31°N, longitude 4.34°E) and the virtual height of the electron density (*h'F2*) response during the period of low solar activity using the analytical methods of relative standard deviation (V_R) for f_oF2, as well as monthly mean for *h'F2*. Apart from the average (μ) and standard deviation (σ) investigated in some previous works, Kouris and Fotiadis (2002) used other analytical parameters (e.g. upper/lower quartiles or deciles which stand for the data scatter) to demonstrate the f_oF2 variability. The latter statistical methods have the benefit of data probability interpretations. Nonetheless, a better measure of the average deviation for each hour of the day from the monthly mean provides the relative standard deviation, yet in terms of probability, it portends awkward interpretation.

MATERIALS AND METHODS

Data and Method of Analysis

Data used for this work consists of ionospheric F2-region critical frequency (f_oF2) and virtual height (*h'F2*). Hourly values of this parameter were extracted from Ilorin (latitude 8.31°N, longitude 4.34°E, dip latitude 2.95°), a low latitude ionospheric station in Nigeria, West Africa. A period of low solar activity, which is the year 2010, is used for this work. The data sets for f_oF2 and *h'F2* were obtained from the ionograms produced by the Ilorin digisonde. The ionograms downloaded from the Digital ionogram Data Base (DIDBase) were manually edited with the SAO Explorer software package. The occurrence probability is the number of F2-region occurrence in a certain hour divided by the number of noticed ionograms in this hour for a month. The digisonde sounds every 15 minutes; this time is so small to reveal the changes we want to study. An hourly interval datasets of F2-region critical frequency (f_oF2) and the virtual height (*h'F2*) was therefore used for the study. In practice, Iheonu and Oyekola (2006) and Chaitanya *et al*. (2012), show that ionospheric variations in the Africa sector located in the Northern Hemisphere are categorised into the seasons of June Solstice, December Solstice, or Equinoctial period. For this purpose, data for the months of April and October represent the equinoctial period; the average across each hour of the two months is used as equinox season. Because Ilorin falls in the Northern Hemisphere, data for the months of July are used for the June Solstice season, while November data falls in the December Solstice season. Each data set covers the whole 24 hours of the day for each of the chosen months of the year 2010 used. This was done in order for we to have a better statistical illustration for the period of low solar activity representation. The thought of using representative months for each of the seasons and their results well presented were earlier adopted by some researchers, such as, Radicella and Adeniyi (1999); Anderson *et al*. (2006); Oladipo *et al*. (2009); Ehinlafa and Adeniyi, (2012); Ehinlafa *et al*. (2023).

Following the illustration of Rishbeth and Mendillo (2001), and also, that of Bilitza *et al*., (2004) and the references therein, we have used the monthly mean (μ) and standard deviation (σ) to calculate the monthly relative deviation, thinking that the variations will show actual changes in critical frequency (f_oF2) and not only meet an existing plasma redistribution. The regular way of quantifying precision is by standard deviation (σ), and hence, it is a precise act of estimating the average; which indicates how well the respective dataset agrees with each other. The standard deviation is expressed mathematically as:

$$\sigma = \sqrt{\frac{\sum_{i=1}^{n}(x_i-\mu)^2}{n-1}} \quad (1)$$

where μ stand for the data mean value, x_i stand for the respective data point, n is taken as the data points number, and $(x_i-\mu)$ represents the deviation from the average of each data point. The precision as a percentage of the average yield the expression of relative standard deviation V_R . A smaller relative standard deviation indicate that the data are more precise. In this study, the estimating f_oF2 relative standard deviation V_R is expressed as:

$$V_R = \frac{\sigma}{\mu} \cdot 100\ \% \quad (2)$$

For the seasonal patterns of the f_oF2 relative deviation and *h'F2* response, we made use of the hourly mean values for the chosen months. In a similar manner, we found the average monthly values across each hour to interpret the annual pattern

RESULTS AND DISCUSSION

Ionospheric f_oF2 Variability

Figure 1 highlights the diurnal f_oF2 relative deviation [V_R (%)] variations plotted versus local time (LT) over Ilorin. On the average, the diurnal patterns follow the same variation for the entire seasons. The relative deviation is noticed to be lowest during the sunrise period (2-32%). After sunset, the relative deviation had increased (8-57%). However, the highest magnitudes were obtained during the pre-sunrise period, with a peak occurring around 0500 LT with a magnitude range of 17-68%. For this pre-sunrise peak, the highest occurred during June Solstice (68%); then Equinox (49%), and the lowest during December Solstice (17%), at low solar activity. A broader range of variation was observed for the entire season during sunrise period of 0600 and 1800 LT with a magnitude of 14-32% just before sunset. The post-sunset peak was noticed between 2100 and 2200 LT during all seasons. For this post-sunset peak, the lowest was noticed in December Solstice (30%) around 2200 LT, followed by June Solstice (46%) around 2200 LT, and the highest in equinoctial season (55%) around 2100 LT. In all the seasons, the post-sunset peak is less than the pre-sunrise peak. Moreover, the daytime relative deviation index notices were seen to be smaller than the nighttime notices. The daytime observation is different from the nighttime observation due to the higher mean (μ) value during the day, which when compared with absolute relative deviation reduces to smaller percentage of relative deviation at daytime (e.g. Bilitza *et al*., 2004).

As reported by Chou and Lee (2008), Oladipo *et al*. (2008), Adebesin *et al*.(2014), Diabaté *et al*. (2019) and Ehinlafa *et al*. (2023), the observation of two f_oF2 relative deviation peaks noticed are attributed to the triggering of the solar ionization onset and turn-off yielding the steep electron density gradients, and also, bringing about the spread-F super-imposition on the electron density background. The pre-sunrise peak was attained lately during December Solstice, and early in June Solstice. The highest post-sunset peak magnitude was noticed during equinoctial season. The observations of f_oF2 variations noticed during the June Solstice is inferred that there could be some other factors existing in this season necessarily causing the relative deviation which may not be existing in other seasons.

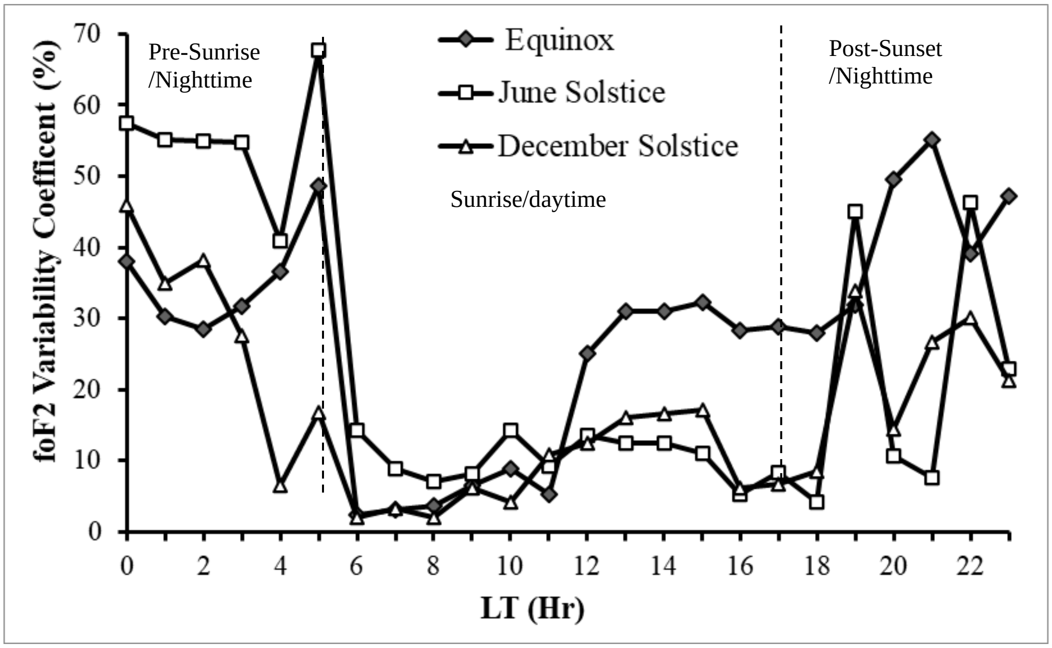

Figure 1: Seasonal Plots of foF2 variability (V_R) over Ilorin during year of low solar activity

The hourly annual plot of variability or relative deviation index (V_R) against local time (LT) is shown in fig. 2. The plot depicts a mean pre-sunrise peak of 44% magnitude around 0500 LT. The sunrise magnitude ranges from 4-20% between the local time of 0600 - 1600, while the post-sunset peak recorded 37% magnitude around 1900 LT. Annually, daytime variability is smaller than the nighttime variation. According to Ambili *et al.* (2012) and the references therein, Alagbe (2012) and Bai *et al.* (2020), gravity waves and irregular wind had also been recommended as another factor causing the enhancement of nighttime electron density gradient.

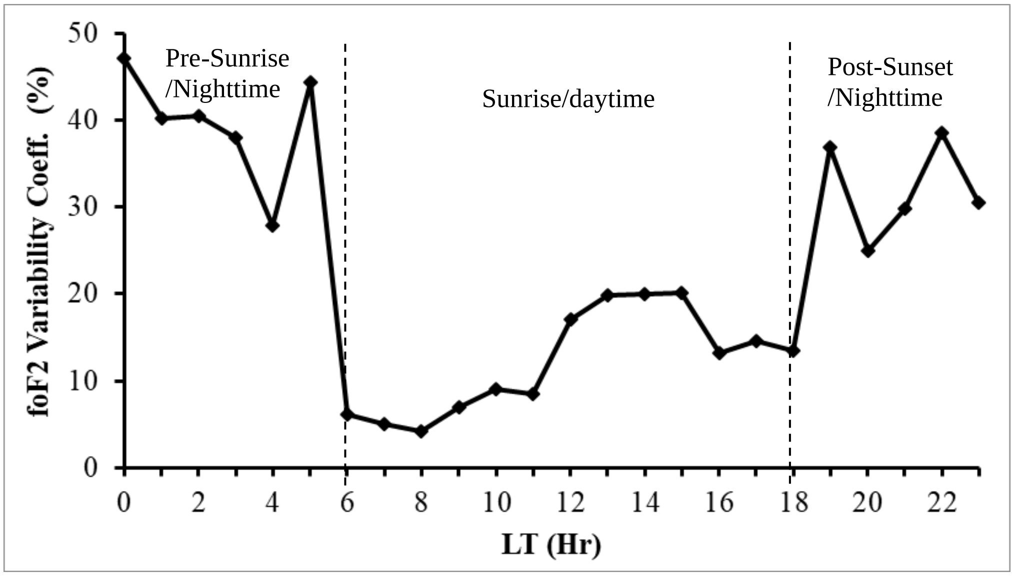

Figure 2: foF2 variability index (V_R) Annual mean plot derived over all seasons for low solar activity

Seasonal h′F2 Observations

Depicted in figure 3 is the corresponding mean seasonal F2-region virtual height. The *h'F2* observations show a gradual rise for the seasons of equinox and December solstice and a sharp growth is indicated for the season of June Solstice within the sunrise period of 0600–1600 LT. During the sunrise period, a noontime peak occurred between 1100 and 1300 LT having a ranging magnitude of 321–410 km for all seasons. The least *h'F2* noontime peak was observed in Equinox (magnitude: 321 km) around 1300 LT and the highest *h'F2* noontime peak was in June Solstice (magnitude: 410 km) around 1200 LT, at low solar activity. It is adjudged that the beefed-up plasma drift in June Solstice season relocates to a higher height the plasma where the loss due to recombination gets much weaker; the plasma found in higher heights thus indicate a lifetime yearning, and then yields a higher magnitude in June Solstice, which is in harmony with Chen *et al*., 2008. Just before sunset, witnessing of a sharp growth was noticed between 1600–1900 LT at all season to attain a *h'F2* second peak (post-sunset peak) except during June solstice. During nighttime period, a post-sunset peak of *h'F2* was recorded between 1900 and 2100 LT for the entire season. However, the highest *h'F2* magnitude was recorded in December Solstice (329 km) around 1900 LT and the least *h'F2* magnitude was noticed in June Solstice (253 km) around 2100 LT. According to Adebesin *et al*. (2013a), the correlation between h_mF2 and the F2-region vertical drift positivity found during the nighttime between 1800 and 2100 LT may be face-saving in symbolising the post-sunset peak of *h'F2* around 1900 and 2100 LT here. Subsequently this time-interval, observing of a sharp fall in the seasonal patterns up till 0400 LT having a ranging magnitude of 234–307 km. Around 0500 LT, a pre-sunrise peak of *h'F2* was recorded, having a magnitude range of (228–318) km for all seasons. The least *h'F2* pre-sunrise peak was noticed in December Solstice (magnitude: 228 km) and the highest *h'F2* pre-sunrise peak was in June Solstice (magnitude: 307 km) at low solar activity. The divergences between the pre-sunrise peaks and the post-sunset peaks become pronounced during the June Solstice.

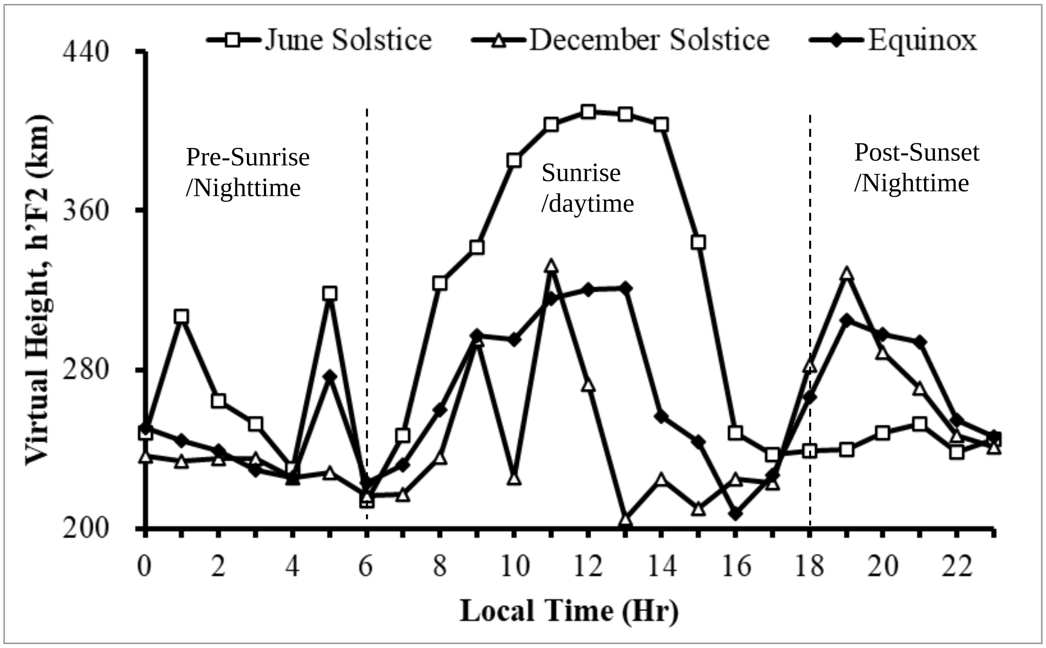

Figure 3: Mean Seasonal Virtual Height of the F2-Region Electron Density during Low Solar Activity

Highlighted in figure 4 is the mean hourly annual virtual height of the F2-region electron density shown similar to fig. 3. The post-sunset peak of an average magnitude 295 km around 1900 LT, which is greater than the pre-sunrise peak with an average magnitude of 275 km around 0500 LT was observed in figure 4 for the *h'F2* annual variation for the condition of this LSA period during the entire season. Also, a noontime peak of *h'F2* annual variation was noticed with a magnitude of 345 km around 1100 LT for all seasons at LSA.

Annually, the daytime variation in *h'F2* creates a valley between the local time of 0900 and 1100 LT which is higher than the one created between 1500 and 1800 LT. *h'F2* nighttime continuous sharp drop around 1900 LT after sunset until a pre-sunrise minimum time around 0500 LT was observed for all seasons. According to Ambili *et al.* (2012) and the references therein, Adebesin *et al.* (2014) and Bai *et al.* (2020), the enhancement of nighttime ionospheric density gradient also shows concurrent rise in *h'F2* magnitudes due to vertical plasma drift during the period of post-sunset resulting from the low recombination loss rate region of electrons relocating rapidly away from the equator.

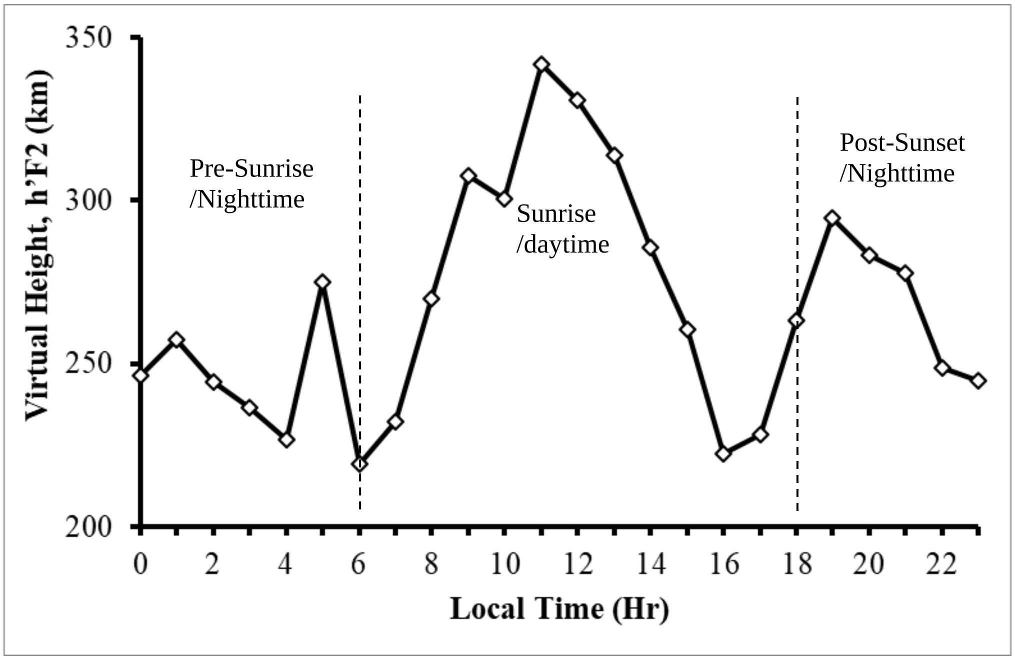

Figure 4: Average Hourly Annual Virtual Height of the F2-Region Electron Density for Solar Minima

CONCLUSION

The investigation of the diurnal, seasonal, and annual f_oF2 relative deviation and the F2-region virtual height response over a West Africa sector equatorial station during a low solar activity period was studied.

Relative deaviation (V_R) is lowest during the sunrise ranging from 2–32%, thereafter V_R increases during the post-sunset ranging from 8-57%, and the highest value were obtained during pre-sunrise (around 0500 LT) ranging from 17-68% for the LSA year. Two main peaks: the pre-sunrise and the post-sunset were noticed. The lowest pre-sunrise peak magnitudes were attained in December Solstice, while the highest magnitudes were obtained during the June Solstice at low solar activity. The increasing V_R pre-sunrise peak magnitudes of 17%, 49% and 68% were recorded respectively during the December Solstice, Equinox and June Solstice seasons. Pre-sunrise peak of relative deviation (V_R) is greater than the post-sunset peak of relative deviation (V_R) during the LSA. During sunrise period, magnitudes of V_R ranges from 14–32% for all seasons during the LSA year.

Annually, V_R peaks were recorded as 44% and 37% magnitudes for the pre-sunrise and the post-sunset respectively. The inverse relation of V_R increasing for all seasons during the LSA is also perpetual during the sunrise period but with smaller implicit effect. These were caused by the solar ionization onset and turn-off on the electron density background due to the assigning of sharp density gradients; as the order of hours for a free electron lifetime is seen to be of importance [Hines *et al*. (1965) and Olga (2021)]. Therefore, the movements of electrons can be strongly subjected by the ionization equilibrium resulting from forces of electromagnetism, temperature differences and distribution.

A *h'F2* pre-sunrise peak with a magnitude range of (228–318) km around 0500 LT during the pre-sunrise period while during the post-sunset period, a peak of post-sunset *h'F2* with a magnitude range of (253–329) km between 1900 and 2100 LT was observed for all seasons during this period of LSA. The divergences between the pre-sunrise peaks and the post-sunset peaks become pronounced during the June Solstice.

After sunset as shown in fig. 3 indicates that there is enhancement in *h'F2* during the nighttime. This observation depicts a state of lower recombination loss rate that is responsible for the relocation of ions, and also, which sustained the elongated period of electron density. Yet, from our plots in fig. 1, a drop-off in electron density were evidently noticed. The sudden depletion in rapidly moving electrons caused by upward plasma drift is responsible for the peak of post-sunset noticed in the equatorial ionosphere.

Annual peaks in f_oF2 relative deviation index as well as in *h'F2* variation plots have indicatively shown that the ionospheric wind and the enhanced plasma drifts serve as controlled mechanism which validates some previous research works..

ACKNOWLEDGEMENTS
The authors appreciate Digisonde owners and international ionogram scaling teams for making available Ilorin data (latitude 8.31°N, longitude 4.34°E, dip latitude 2.95º) from the Digital ionogram DataBase (DIDBase) online site for possible use in this study. O. E. Ehinlafa, one of the authors, express his gratitude to the Editors for the nice job of editing the original manuscript.

REFERENCES
Adebesin, B.O., Adekoya, B.J., Ikubanni, S.O., Adebiyi, S.J., Adebesin, O.A., Joshua, B.W., and Olonade, K.O., (2014) Ionospheric foF2 Morphology, response of F2-Layer Height over Jicarmarca during different solar epochs and comparison with IRI-2012 model; *J. Earth Syst. Sci.* **123(4),** 751–765.

Adebesin, B.O., Adeniyi, J.O., Adimula, I.A., Reinisch, B.W., and Yumoto, K., (2013a) Equatorial vertical plasma drift velocities and electron densities inferred from ground-based ionosonde measurements during low solar activity; *J. Atmos. Sol. Terr. Phys.* **97,** 58–64, https://doi.org/10.1016/j.jastp.2013.02.010.

Alagbe, G. A. (2012) Geomagnetic storm effects on F2 layer peak electron density and other profile parameters at high solar activity at an equatorial station; *J. Phys. Sci. Innovation*, **4,** 5–12, ISSN 2277–0119

Ambili, K. M., St-Maurice, J. P. and Choudhary, R. K. (2012) On the sunrise oscillation of the F region in the equatorial ionosphere; *Geophys. Res. Lett.*, **39,** L16102, https://doi.org/10.1029/2012GL052876

Anderson, D., Anghel, A., Chau, J., Yumoto, K., Bhattacharyya, A. and Alex, S. (2006) Daytime, low latitude, vertical E×B drift velocities, inferred from ground-based magnetometer observations in the Peruvian, Philippine and Indian longitude sectors under quiet and disturbed conditions; *ILWS WORKSHOP, GOA*, February 19–24, 2006, pp. 1–6

Bai, H., Feng, F., Wang, J. A. (2020) Combination Prediction Model of Long-Term Ionospheric foF2 Based on Entropy Weight Method. *Entropy*, *22*, 442

Bilitza, D., Altadill, D., Zhang, Y., Mertens, C., Truhlik, V., Richards, P., McKinnell, L.A. and Reinisch, B. (2014) The International Reference Ionosphere 2012—A Model of International Collaboration. *Journal of Space Weather and Space Climate*, 4, A07 https://doi.org/10.1051/swsc/2014004

Chaitanya, P. P., Patra, A. K. and Rao, V. B. (2012) Contrasting features of the F3 layer during high and low solar activity conditions observed from Indian low latitude; *Indian J. Radio Space Phys.*, **41,** 121–129

Chou, Y. T. and Lee, C. C. (2008) Ionospheric variability at Taiwan low latitude station: Comparison between observations and IRI 2001 model; *Adv. Space Res.*, **42,** 673–681

Diabaté, A., Zerbo, J. L. and Ouattara, F. (2019) Variation of the foF2 Parameter during Fluctuating Activity: Prediction with IRI-2012 Compared to Measured Data from Ouagadougou Ionosonde Station during Solar Cycles 21 and 22; *Vietnam Journal of Earth Sciences*, 41, 69-78

Ehinlafa, O. E. and Adeniyi, J. O. (2012) Equatorial M(3000)F2 Estimation of F2-Layer Peak Heights During Low Solar Activity, *Advances in Space Research Journal*, 49(4); 711 – 715. https://doi.org/10.1016/j.asr.2011.11.031

Ehinlafa, O. E., Johnson, M. J., Àlàgbé, G. A., Ige, S. O. and Adeniyi, J. O. (2023) Morphology of Ionospheric f_oF2 and N_mF2 over Ilorin during Low Solar Epochs. Mountain Top University Journal of Applied Science and Technology, 3(1), 71 - 79

Hines, C. O., Paghis I., Hartz, T. R. and Fejer, J. A. (eds) (1965) *Physics of the Earth's Upper Atmosphere*; Prentice-Hall, Inc. Englewood Cliffs, N.J.

Iheonu, E. E. and Oyekola, O. S. (2006) Vertical drift velocity in the daytime F-region at Ibadan estimated from ionosonde data; *Indian J. Radio Space Phys.*, **35(1),** 9–13.

Jayachandran, B., Balachandran, N. R., Balan, N. and Rao, P.B., (1995): Short time variability of the ionospheric electron content and peak electron density during solar cycles for a low latitude station, *J. Atmos. Sol. Terr. Phys.* **52**, 1599-1605

Jin, S. G., Luo, R. J. and Park, P. (2008) GPS observations of the ionospheric F2-layer behaviour during the 20th November 2003 geomagnetic storm over South Korea; *J. Geodesy*, **82,** 883–892.

Kouris, S. S. and Fotiadis, D. N. (2002) Ionospheric variability: A comparative statistical study; *Adv. Space Res.*, **29(6),** 977–985.

Lilensten, J. and Blelly, P. L. (2002) The TEC and F2 parameters as traces of the ionosphere and thermosphere; *J. Atmos. Sol. Terr. Phys.*, **64,** 775–793

Oladipo, O. A., Adeniyi, J. O., Radicella, S. M. and Obrou, O. K. (2008) Variability of equatorial ionospheric electron density at fixed heights below the F2 peak; *J. Atmos. Sol. Terr. Phys.*, 70, 1056–1065.

Oladipo, O. A., Adeniyi, J. O. and Radicella, S. M. (20090 Electron density distribution at fixed heights N(h): Gaussian distribution test; *J. Atmos. Sol. Terr. Phys.*, **71,** 1–10

Olawepo, A, O, and Adeniyi, J. O. (2012) Ionosphere's F2-layer response to 2006 geomagnetic storm at Ilorin, Nigeria; *The African Rev. Phys,.* **7(0031),** 277–281.

Olga, M., (2021) The Influence of Space Weather on the Relationship between the Parameters TEC and foF2 of the Ionosphere, *IEEE J. Radio Freq. Identify*, 5, 261 - 268

Ouattara, F. (2013) IRI-2007 foF2 Predictions at Ouagadougou Station during Quiet Time Periods from 1985 to 1995. Archives of Physics Research, 4, 12-18.

Radicella, S.M. and Adeniyi, J.O. (1999) Equatorial ionospheric electron density below the F2 peak. *Radio Science*, **34**(5), 1153- 1163.

Risbeth, H. and Mendillo, M. (2001) Pattern of F2-layer variability; *J. Atmos. Sol. Terr. Phys.*, **63(15),** 1661–1680

Zhang, S. R. and Holt, J. M. (2008) Ionospheric climatology and variability from long-term and multiple incoherent scatter radar observations: Variability; *Ann. Geophys.*, **26,** 1525–1537